Low-moment magnetism in the double perovskites Ba_2MOsO_6 ($M =$ Li,Na)

Andrew J. Steele,[1] Peter J. Baker,[2] Tom Lancaster,[1] Francis L. Pratt,[2] Isabel Franke,[1] Saman Ghannadzadeh,[1] Paul A. Goddard,[1] William Hayes,[1] D. Prabhakaran,[1] and Stephen J. Blundell[1,*]

[1]*Oxford University Department of Physics, Clarendon Laboratory, Parks Road, Oxford OX1 3PU, United Kingdom*
[2]*ISIS Pulsed Neutron and Muon Source, Science and Technology Facilities Council, Rutherford Appleton Laboratory, Didcot OX11 0QX, United Kingdom*

The magnetic ground states of the isostructural double perovskites Ba_2NaOsO_6 and Ba_2LiOsO_6 are investigated with muon-spin relaxation. In Ba_2NaOsO_6 long-range magnetic order is detected via the onset of a spontaneous muon-spin precession signal below $T_c = 7.2 \pm 0.2$ K, while in Ba_2LiOsO_6 a static but spatially disordered internal field is found below 8 K. A probabilistic argument is used to show from the observed precession frequencies that the magnetic ground state in Ba_2NaOsO_6 is most likely to be low-moment ($\approx 0.2\mu_B$) ferromagnetism and not canted antiferromagnetism. Ba_2LiOsO_6 is antiferromagnetic and we find a spin-flop transition at 5.5 T. A reduced osmium moment is common to both compounds, probably arising from a combination of spin-orbit coupling and frustration.

I. INTRODUCTION

Metal oxides containing $5d$ transition-metal ions provide a wealth of novel magnetic behavior in which orbital, charge, and spin degrees of freedom play a role. The varied properties observed are due in part to the extended character of the $5d$ orbitals, reducing the effects of electron correlation. Moreover, the larger spin-orbit coupling in $5d$ oxides contributes to a balance of competing energy scales substantially different from that in the more familiar $3d$ transition-metal oxides. In this context, osmium compounds provide a number of interesting examples. Though OsO_2, $SrOsO_3$, and $BaOsO_3$ [all containing Os^{4+} ($5d^4$)] are Pauli paramagnets,[1] double perovskites of the form $Ba_2(Na,Li)OsO_6$ [containing Os^{7+} ($5d^1$), with ions arranged on a face-centered-cubic (fcc) lattice] exhibit Mott-insulating, $S = \frac{1}{2}$ local-moment behavior.[2,3] However, the insulator barium sodium osmate (Ba_2NaOsO_6) has drawn particular attention[4] due to its seemingly contradictory combination of negative Weiss temperature (≈ -10 K) and yet weak ferromagnetic moment ($\approx 0.2\mu_B$/formula unit) below $T_c \approx 7$ K. This contrasts with the isostructural Ba_2LiOsO_6, which has both a negative Weiss temperature and no ferromagnetic moment.[2,5] The high-temperature paramagnetic moment $\mu_{eff} \approx 0.6\mu_B$ in Ba_2NaOsO_6 is also indicative of substantial spin-orbit coupling.[4]

The double-perovskite structure of Ba_2NaOsO_6 is shown in Fig. 1(a); note that sodium and osmium ions inhabit alternate oxygen octahedra. The negative Weiss constant raises the possibility that the material is a canted antiferromagnet, although first-principles density functional theory electronic structure calculations indicate that a ferromagnetic state has lower energy.[6] The large hybridization between the osmium $5d$ and oxygen $2p$ orbitals leads to a very large crystal-field splitting (several eV) between the e_g and t_{2g} bands. It has been suggested that the low moment arises from a partial cancellation of orbital and spin angular momenta in the occupied spin-up t_{2g} band.[6] A ferromagnetic phase in ordered double perovskites (with moments along [110]) is also predicted from a mean-field treatment of the orbital-dependent exchange for certain values of parameters in a

model Hamiltonian.[7] An alternative mechanism[8] involves the frustration of both the antiferromagnetic interactions and the orbital ordering by the fcc lattice, resulting in a delicate balance of interactions which favors ferromagnetism for Ba_2NaOsO_6, but antiferromagnetism for Ba_2LiOsO_6. In view of these competing explanations, further experimental data which can distinguish between different magnetic configurations are desirable. We have used muon-spin relaxation (μ^+SR) as a local probe of magnetism in Ba_2NaOsO_6, and find that our data are consistent with the development of long-range ferromagnetic order with a reduced moment. A similarly reduced moment is likely for Ba_2LiOsO_6.

II. EXPERIMENTAL

Crystallites of Ba_2NaOsO_6 and Ba_2LiOsO_6 were grown using a flux method.[2] Powders of Os (99.8%), $Ba(OH)_2\cdot8H_2O$ (98%), and high-purity $NaOH\cdot H_2O$ (99.996%) or LiOH (99.995%) and KOH (99.99%) were mixed in the ratio 1:2.1:300 or 1:2.1:140:75, respectively. These mixtures were each placed in an alumina crucible inside a thick quartz tube which was inserted into a 600 °C preheated tube furnace where it was held for three days. The furnace was then rapidly cooled to room temperature and small single crystals were harvested from each crucible. Our muon experiments used a very large number of these crystals without alignment. Magnetization [Fig. 1(b)] and susceptibility (not shown) measurements using a superconducting quantum interference device (SQUID) magnetometer are consistent with earlier work[2,4] but also reveal a spin-flop transition in Ba_2LiOsO_6 at around 5.5 T. Pulsed field magnetometry revealed no additional transitions up to 45 T [Fig. 1(c)].

In a μ^+SR experiment,[9] spin-polarized positive muons are implanted into a sample. The muons usually stop in sites with high electron density. Their spins precess around the local magnetic field with a frequency $\nu = \gamma_\mu|B|/2\pi$, where $\gamma_\mu = 2\pi \times 135.5$ MHz T^{-1} is the muon gyromagnetic ratio. Muons are unstable with mean lifetime 2.2 μs, and decay into a positron and two neutrinos, the former being preferentially
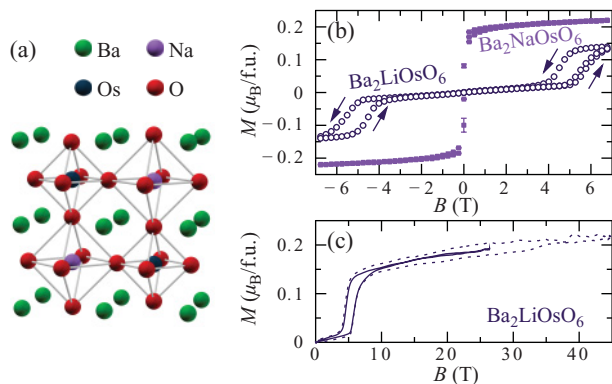
FIG. 1. (Color online) (a) Double-perovskite crystal structure. Alternation of OsO_6 octahedra (top left and bottom right) and NaO_6 octahedra, with barium ions occupying the remaining space. (b) Magnetization measured at 2 K in a SQUID magnetometer for Ba_2MOsO_6. (c) Magnetization measured at 4 K in pulsed field for Ba_2LiOsO_6, calibrated against the SQUID magnetization data. Data from a 45 T shot (dashed line) are noisier than those from a 25 T shot (solid line) but show no evidence for additional magnetic transitions.

FIG. 2. (Color online) Muon data above and below the magnetic transition for (a) Ba_2LiOsO_6 and (b) Ba_2NaOsO_6. The inset to (a) shows the temperature dependence of the Gaussian relaxation rate in Ba_2LiOsO_6 (the solid line is a best fit to a phenomenological $[1 - (T/T_N)^\alpha]^\beta$ form; see text). The 1.5 K data in (a) can be fitted to either an exponentially damped Kubo-Toyabe function (green dashed line) or an exponentially damped oscillation plus a fast-relaxing component (black solid line). Fits in (b) are described in the text.

emitted along the direction of muon spin. Detectors record the direction of positron emission, whose time dependence tracks the ensemble of muon spins rotating around their respective local **B** fields. In these experiments, the detectors are divided into a forward (F) and backward (B) detector bank, and the direction of preferential positron emission is represented by the asymmetry between $N_F(t)$ and $N_B(t)$, the number of positrons detected in each detector bank as a function of time. The asymmetry function, which is proportional to the spin polarization of the muon ensemble, is defined as $A(t) = [N_F(t) - \alpha N_B(t)]/[N_F(t) + \alpha N_B(t)]$, where α is an experimentally determined parameter dependent on apparatus geometry and detector efficiency.

Our μ^+SR measurements were performed using the General Purpose Surface-Muon Instrument at the Swiss Muon Source (SμS), Paul Scherrer Institut, Switzerland. Samples were wrapped in 25 μm Ag foil and mounted on a "flypast" holder comprising two silver prongs, thereby minimizing the background signal.

III. RESULTS

Typical zero-field μ^+SR spectra measured above and below the transition temperature T_c are shown in Fig. 2 for both Ba_2LiOsO_6 and Ba_2NaOsO_6. For Ba_2LiOsO_6, a single, heavily damped oscillation is present at low temperature, signifying a static but spatially disordered spontaneous field. At higher temperature the relaxation is Gaussian, signifying the paramagnetic state. Focusing only on the early-time relaxation and plotting the relaxation rate (crudely parametrizing the development of static fields) as a function of temperature [inset to Fig. 2(a)] displays the magnetic transition at 8 K. For Ba_2NaOsO_6, two damped oscillations are clearly visible at low temperature, demonstrating the existence of a transition to a state of long-range magnetic order. Just above the transition the relaxation is exponential [Fig. 2(b)] but becomes Gaussian
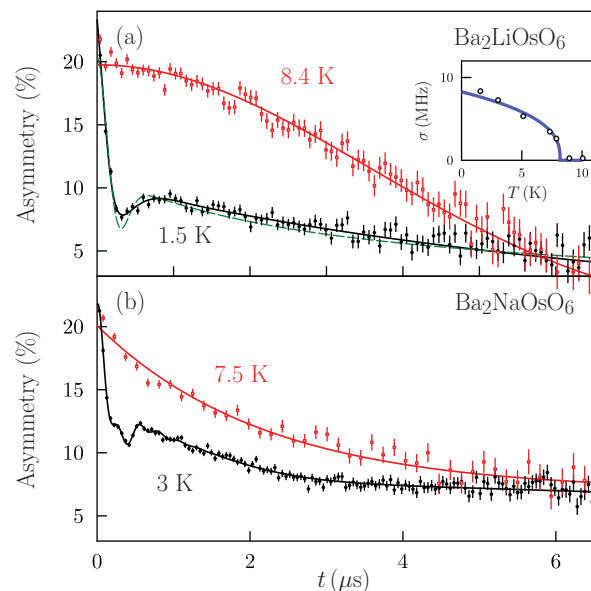
at higher temperatures (not shown). Data below the transition were fitted to

$$A(t) = \left[\sum_{i=1}^{2} A_i e^{-\lambda_i t} \cos 2\pi \nu_i t + A_3 e^{-\lambda_3 t}\right] + A_0 e^{-\lambda_0 t},$$
(1)

where the terms in square brackets represent muons which stop inside the sample. These comprise two oscillatory components (reflecting those components of the initial muon-spin polarization aligned transverse to the direction of the quasistatic local magnetic field at the muon sites) and a nonoscillatory component. The final term in Eq. (1) accounts for a background signal from those muons that stop in the silver sample holder or cryostat tails. The frequencies of the two oscillatory components were held in fixed proportion $\eta = \nu_2/\nu_1$ during fitting (thus we will now write $\nu_1 \equiv \nu$ and $\nu_2 \equiv \eta\nu$). The existence of two oscillatory components most likely indicates two crystallographically similar muon sites, perhaps one nearer to the magnetic Os ion and the other nearer the nonmagnetic Na ion. The ratio of the probabilities of stopping in the two oscillating states is $A_2/A_1 = 0.19 \pm 0.02$. Our fits yield $A_3/A_2 = 0.92 \pm 0.01$, $\nu(T \to 0) = 3.9 \pm 0.1$ MHz, and $\eta = 0.4 \pm 0.05$. The relaxation rate $\lambda_1 \approx 2$ MHz at low temperature and diverges as the transition is approached from below. The second frequency is more strongly broadened; we find $\lambda_2 \approx 4$ MHz, which does not vary significantly as a function of temperature. λ_3 decreases from 1.6 ± 0.1 MHz at 1.5 K
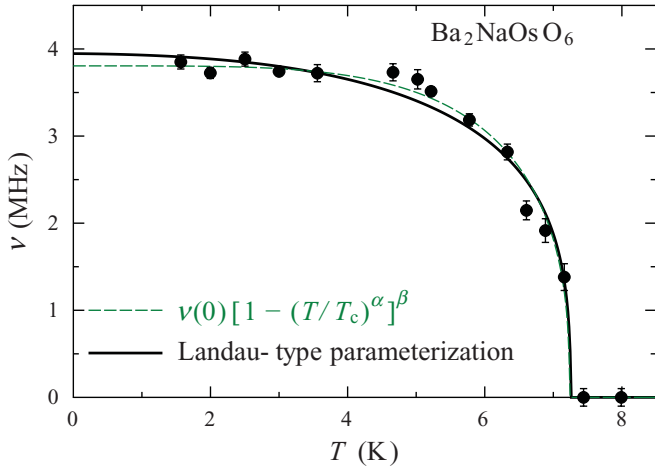
FIG. 3. (Color online) The frequency $\nu(T)$ extracted from fits to $A(t)$ spectra as a function of sample temperature T, along with fits to various models (see text). Data are only shown for the larger frequency ν_1 because ν_2 was held in fixed proportion during fitting (see text).

toward zero at the transition temperature T_c. The temperature dependence of ν was fitted to the phenomenological form

$$\nu(T) = \nu(0)[1 - (T/T_c)^{\alpha}]^{\beta}, \qquad (2)$$

with β fixed at 0.367, corresponding to the three-dimensional Heisenberg model, yielding $T_c = 7.2 \pm 0.2$ K (Fig. 3). A similarly good fit can be obtained using a Landau-type parametrization of the equation of state of a ferromagnet [using Eq. (18) of Kuz'min[10] with parameters appropriate for Fe], yielding the same estimate of T_c. The agreement with these latter two models is consistent with three-dimensional ferromagnetic order.

IV. DISCUSSION

The data extracted from a μ^+SR experiment can be used to infer further information about the nature of the magnetically ordered state by examining the local field at the muon site. Since the positive muon seeks out areas of negative charge density, constraints can be placed on the likely location of stopped muons. Calculating the magnetic field at these plausible muon sites and comparing it to $|\boldsymbol{B}| = 2\pi \nu_i(0)/\gamma_\mu$, allows the consistency of a suggested magnetic structure and experiment to be checked. The magnetic field $\boldsymbol{B}_{\text{local}}$ at the muon site is given by

$$\boldsymbol{B}_{\text{local}} = \boldsymbol{B}_0 + \boldsymbol{B}_{\text{dipole}} + \boldsymbol{B}_{\text{L}} + \boldsymbol{B}_{\text{demag}} + \boldsymbol{B}_{\text{hyperfine}}, \qquad (3)$$

where $\boldsymbol{B}_0$ represents the applied field (zero in our experiments), $\boldsymbol{B}_{\text{dipole}}$ is the dipolar field from magnetic ions, $\boldsymbol{B}_{\text{L}} = \mu_0 \boldsymbol{M}/3$ is the Lorentz field, $\boldsymbol{B}_{\text{demag}}$ is the demagnetizing field from the sample surface, and $\boldsymbol{B}_{\text{hyperfine}}$ is the contact hyperfine field caused by any spin density overlapping with the muon wave function. The dipolar field $\boldsymbol{B}_{\text{dipole}}$ is a function of the muon site $\boldsymbol{r}_\mu$ and is composed of the vector sum of the fields from each of the magnetic ions in the crystal, so that

$$\boldsymbol{B}_{\text{dipole}}(\boldsymbol{r}_\mu) = \mu \sum_i \frac{\mu_0}{4\pi r^3}[3(\hat{\boldsymbol{\mu}}_i \cdot \hat{\boldsymbol{r}})\hat{\boldsymbol{r}} - \hat{\boldsymbol{\mu}}_i], \qquad (4)$$
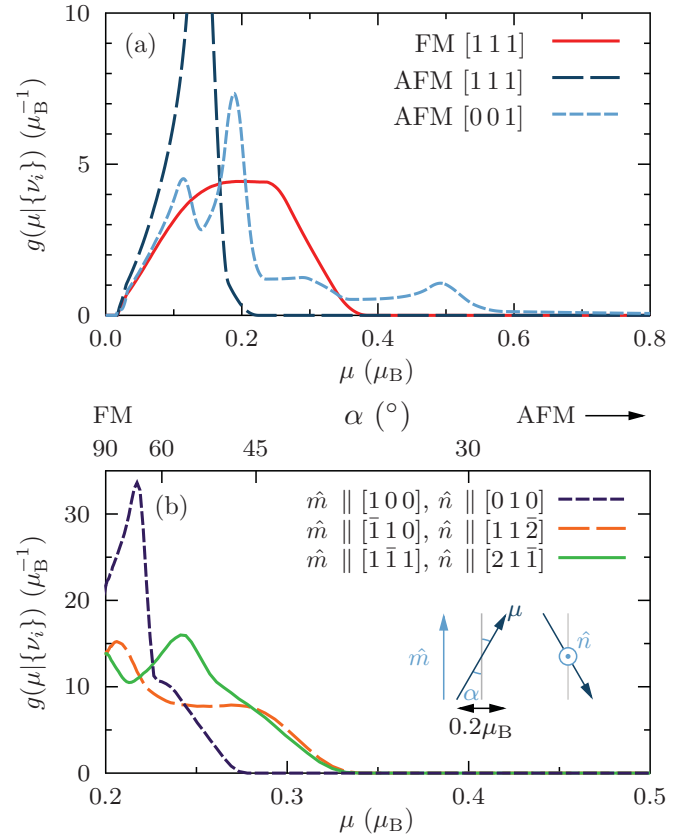

FIG. 4. (Color online) (a) Probability density functions (PDFs) of the moment (μ) on the Os site in Ba_2NaOsO_6 inferred by Bayes' theorem from dipole-field simulations using representative trial magnetic structures (FM, ferromagnetic; AFM, antiferromagnetic) and the experimentally observed frequencies. (b) PDFs evaluated using the constraint of a fixed ferromagnetic component $\mu \sin\alpha = 0.2\mu_B$. Inset shows the assumed structure: antiferromagnetic moments along $\hat{\boldsymbol{m}}$ rotated as shown by an angle α about $\hat{\boldsymbol{n}}$.

where $\boldsymbol{r} = \boldsymbol{r}_i - \boldsymbol{r}_\mu$ is the relative position of the muon and the ith ion with magnetic moment $\boldsymbol{\mu}_i = \mu\hat{\boldsymbol{\mu}}_i$, and the sum is evaluated over a large sphere centered at $\boldsymbol{r}_\mu$.

Dipole field simulations were performed for Ba_2NaOsO_6 using a variety of magnetic models: ferromagnetism and antiferromagnetism (ignoring any canting) with moments oriented along [001], [011], and [111]. The muon site is not known and so we adopt a probabilistic approach.[11] The metal ions in this system are all positively charged, meaning that the muon is unlikely to stop near them. In other oxides, muons have been shown to stop around 0.1 nm from an O^{2-} ion.[12] In our calculations, positions in the unit cell were generated at random and dipole fields calculated at sites which were both approximately this distance from an oxygen ion ($0.09 \leqslant r_{\mu\text{-O}} \leqslant 0.11$ nm) and not too close to a positive ion ($r_{\mu\text{-+}} \geqslant 0.1$ nm). The magnitudes of the resulting fields were then converted into muon precession frequencies, and the resulting histogram yields the probability density function (PDF) $f(\nu/\mu)$, evaluated as a function of precession frequency ν divided by osmium moment μ (since the precession frequency scales with the osmium moment). This analysis ignores contributions from the Lorentz field and demagnetizing field, although these cancel each other to some

extent and we estimate them to be less than 2 MHz. More difficult to estimate is the importance of the contact hyperfine field, $\boldsymbol{B}_{\text{hyperfine}}$, which is neglected. Since the Os^{7+} ion is both small and positively charged, this contribution should not be significant and would be even further reduced if μ is low.

Since ν is obtained from experiment, what we would like to know is $g(\mu|\nu)$, the PDF of μ *given* the observed ν. This can be obtained from our calculated $f(\nu/\mu)$ using Bayes' theorem,[13] which yields

$$g(\mu|\nu) = \frac{\frac{1}{\mu} f(\nu/\mu)}{\int_0^{\mu_{\text{max}}} \frac{1}{\mu'} f(\nu/\mu') \, d\mu'}, \tag{5}$$

where we have assumed a prior probability for the osmium moment that is uniform between zero and μ_{max}. We take $\mu_{\text{max}} = 1\mu_B$, although our results are insensitive to the precise value of μ_{max} as long as it is reasonably large. When multiple frequencies ν_i are present in the spectra, it is necessary to multiply their probabilities of observation in order to obtain the chance of their simultaneous observation, so we evaluate $g(\mu|\{\nu_i\}) \propto \prod_i \int_{\nu_i-\Delta\nu_i}^{\nu_i+\Delta\nu_i} f(\nu_i/\mu) \, d\nu_i$, where $\Delta\nu_i$ is the error on the fitted frequency.

The results of this are shown in Fig. 4(a), and show that for all collinear magnetic structures considered a low μ is overwhelmingly likely. Furthermore, for the ferromagnetic case the most probable is $\mu \approx 0.2\mu_B$, consistent with the magnetization measurements (the AFM structures are also consistent with a low μ, but are ruled out by the magnetization measurements). An alternative method of testing the hypothesis of a reduced moment is to consider possible canted structures in which moments are counter-rotated by an angle α, subject to the constraint that $\mu \sin\alpha = 0.2\mu_B$. The results are shown in Fig. 4(b) and are again consistent with a reduced moment μ, certainly lower than the high-temperature paramagnetic moment.

Thus, this probabilistic methodology suggests that the small magnetic moment of ordered Ba_2NaOsO_6 is likely to be true weak-moment ferromagnetism, rather than an artifact of a canted magnetic structure with larger moments. The moments in Ba_2LiOsO_6 appear to be static but show a larger degree of disorder than those of the Ba_2NaOsO_6 for $T < T_N$. The local field at the muon site (estimated from either the extracted Kubo-Toyabe field distribution width or the damped oscillation frequency) is ~ 0.01 T. A similar Bayesian analysis (not shown) also yields a likely low moment $\lesssim 0.2\mu_B$, consistent with that measured in the spin-flop state [Figs. 1(b) and 1(c)]. Thus a low moment is common to both compounds. In contrast to $BaIrO_3$, which achieves a low ferromagnetic moment due to charge-density wave formation,[14] in these compounds the origin must be rather different. It has been postulated[6,8] that the d^1 spin moment of Os is compensated by the t_{2g} $L = 1$ orbital moment induced by the very strong spin-orbit coupling. Partial orbital quenching by the environment is thought to destroy the perfect compensation of the moment, leading to a small remaining magnetic moment. However, an important complication[7,8] is that the antiferromagnetic orbital-dependent coupling between OsO_6 clusters takes place on an fcc lattice. It is therefore strongly frustrated and may hence be responsible for the sensitivity of the ground state to minor chemical changes, explaining the difference between the magnetic properties of isostructural Ba_2LiOsO_6 and Ba_2NaOsO_6.

---

*s.blundell@physics.ox.ac.uk

[1] J. E. Greedan, D. B. Willson, and T. E. Haas, Inorg. Chem. **11**, 2461 (1968).

[2] K. E. Stitzer, M. D. Smith, and H.-C. zur Loye, Solid State Sci. **4**, 311 (2002).

[3] K. E. Stitzer, A. E. Abed, M. D. Smith, M. J. Davis, S.-J. Kim, J. Darriet, and H.-C. zur Loye, Inorg. Chem. **42**, 947 (2003).

[4] A. S. Erickson, S. Misra, G. J. Miller, R. R. Gupta, Z. Schlesinger, W. A. Harrison, J. M. Kim, and I. R. Fisher, Phys. Rev. Lett. **99**, 016404 (2007).

[5] A. W. Sleight, J. Longo, and R. Ward, Inorg. Chem. **1**, 245 (1962).

[6] H. J. Xiang and M.-H. Whangbo, Phys. Rev. B **75**, 052407 (2007).

[7] G. Chen, R. Pereira, and L. Balents, Phys. Rev. B **82**, 174440 (2010).

[8] K.-W. Lee and W. E. Pickett, Europhys. Lett. **80**, 37008 (2007).

[9] S. J. Blundell, Contemp. Phys. **40**, 175 (1999).

[10] M. D. Kuz'min, Phys. Rev. B **77**, 184431 (2008).

[11] S. J. Blundell, Physica B **404**, 581 (2009); A. J. Steele, T. Lancaster, S. J. Blundell, P. J. Baker, F. L. Pratt, C. Baines, M. M. Conner, H. I. Southerland, J. L. Manson, and J. A. Schlueter, Phys. Rev. B **84**, 064412 (2011).

[12] J. Brewer, R. Kiefl, J. Carolan, P. Dosanjh, W. Hardy, S. Kreitzman, Q. Li, T. Riseman, P. Schleger, H. Zhou, E. J. Ansaldo, D. R. Noakes, L. P. Le, G. M. Luke, Y. J. Uemura, K. Hepburn-Wiley, and C. E. Stronach, Hyperfine Interact. **63**, 177 (1991).

[13] D. S. Sivia and J. Skilling, *Data Analysis: A Bayesian Tutorial*, 2nd ed. (Oxford University Press, Oxford, 2006).

[14] M. L. Brooks, S. J. Blundell, T. Lancaster, W. Hayes, F. L. Pratt, P. P. C. Frampton, and P. D. Battle, Phys. Rev. B **71**, R220411 (2005).